nature neuroscience

A functional circuitry for edge-induced brightness perception

Chou P Hung[1], Benjamin M Ramsden[2] & Anna Wang Roe[3]

The identification of visual contours and surfaces is central to visual scene segmentation. One view of image construction argues that object contours are first identified and then surfaces are filled in. Although there are psychophysical and single-unit data to suggest that the filling-in view is correct, the underlying circuitry is unknown. Here we examine specific spike-timing relationships between border and surface responses in cat visual cortical areas 17 and 18. With both real and illusory (Cornsweet) brightness contrast stimuli, we found a border-to-surface shift in the relative timing of spike activity. This shift was absent when borders were absent and could be reversed with relocation of the stimulus border, indicating that the direction of information flow is highly dependent on stimulus conditions. Furthermore, this effect was seen predominantly in 17–18, and not 17–17, interactions. These results demonstrate a border-to-surface mechanism at early stages of visual processing and emphasize the importance of interareal circuitry in vision.

Vases from China's Song dynasty employed faint contrast borders to imbue an illusory sense of shading on an otherwise equiluminant background (**Fig. 1a**, compare shading of head and arms versus background). This phenomenon, known as edge induction[1,2], is distinct from other brightness illusions[3,4] and probably aids in our detection of objects under nonuniform illumination (for example, under a bush or forest canopy) or near-threshold contrast (for example, when objects are dimly lit or seen through fog), where high-frequency edge information can be the most behaviorally relevant signal. Computer vision algorithms and models of the visual system have incorporated edge induction by propagating information (for example, via diffusion) from border to surface, with the implicit assumption that such propagation indeed occurs in biology[5–7]. Although it is conceivable that no such propagation is necessary and that object surfaces may be sufficiently encoded by edges alone (possibly via banks of spatial frequency filters[8–13]), results from both humans and animals have shown a delayed surface representation that is suggestive of edge induction or filling-in[14–21].

Neuronal evidence of filling-in has been reported in the form of weak changes in the firing rate of surface responses (on the order of a few spikes per second) that are sensitive to the profile of the border region and that tend to be stronger in higher visual areas. It has been unclear whether such responses are due to propagation or feedback and whether the delayed increases in firing rate truly signal surface properties or are a result of propagation of excitability away from the border. To date, physiological evidence for edge induction has been limited to single-cell recordings that suggest a delayed surface response but lack the cell- and context-specificity to infer the underlying functional circuit.

To study the neural underpinnings of edge induction, we have examined the interaction between border and surface representations in cat visual cortex. Based on what is known about the visual processing stream, one hypothesis is that edge induction begins with oriented cells in primary visual cortex (area 17), the first stage of edge extraction[20,22–31]. Such oriented responses are thought to result from the integration of multiple aligned nonoriented inputs from the thalamus[32]. These oriented responses then propagate this border information to the surface representation via unknown mechanisms. An alternative possibility is that surface feature responses are first activated by fast conduction magnocellular inputs, followed by the orientation signal that is obtained by integration of nonoriented inputs[33–34]. Whether border responses precede surface responses or vice-versa[35] and whether the responses are cell- and context-specific are fundamental unanswered questions of the circuitry underlying edge induction. Here, by recording isolated spike activity from pairs of cells, one (in area 17) with receptive field at the contrast border and the other (in area 17 or 18) with receptive field at the stimulus surface, we probed the relative timing of spike activity between border and surface representations.

RESULTS

We examined border-surface interactions under four simple stimulus conditions with the same average overall luminance. These conditions were: Real, Cornsweet (based on the Craik-O'Brien-Cornsweet illusion), Narrow Real and Blank (**Fig. 1b**, and unpublished data, http://www.psy.vanderbilt.edu/faculty/roeaw/edgeinduction). In the 'evoked' conditions (first three conditions), the brightness (perceived luminance) of the two surfaces on either side of a stationary border was sinusoidally counterphased. In the Real condition, surface luminance

[1]Institute of Neuroscience and Brain Research Center, 155 Sec. 2 Li-Nong St., National Yang Ming University, Taipei 112, Taiwan. [2]Department of Neurobiology and Anatomy, Sensory Neuroscience Research Center, West Virginia University School of Medicine, Morgantown, West Virginia 26506, USA. [3]Department of Psychology, Vanderbilt University, 301 Wilson Hall, Nashville, Tennessee 37203, USA. Correspondence should be addressed to A.W.R. (anna.roe@vanderbilt.edu).

Received 12 April; accepted 28 June; published online 19 August 2007; doi:10.1038/nn1948

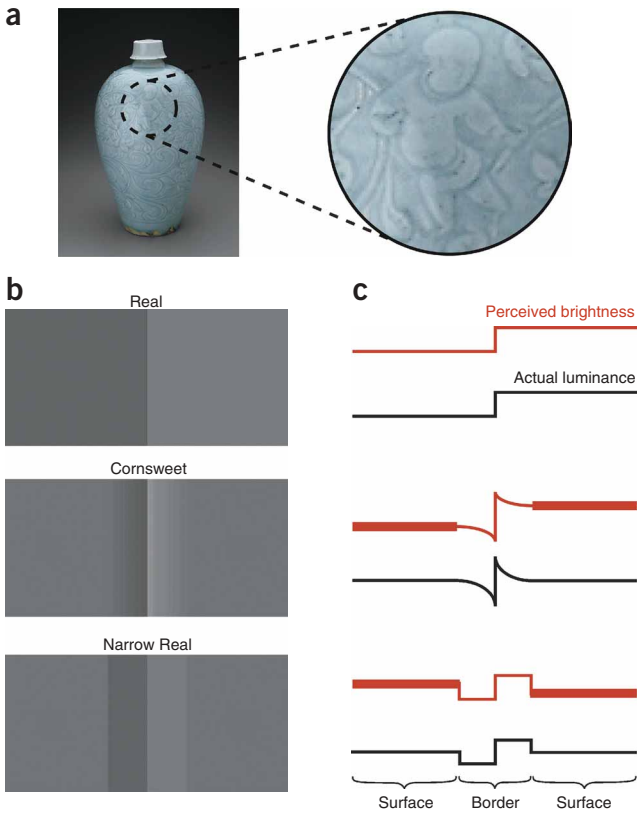

Figure 1 Real and illusory brightness stimuli. (**a**) 12th-century Song dynasty vase, illustrating edge-induction phenomenon. Reprinted with permission, copyright 1999, The Art Institute of Chicago. (**b**) Examples of the Real (top), Cornsweet (middle) and Narrow Real (bottom) stimuli designed to evoke edge induction. (**c**) Luminance (black) and brightness (perceived luminance, red) profiles of the three stimuli. Surfaces in the Cornsweet and Narrow Real conditions were equiluminant and static. Although all three stimuli had the same sign of luminance contrast at the border (lighter on right, darker on left), the Narrow Real stimulus produced a weaker and opposite surface brightness contrast (compare thick red lines for Cornsweet with Narrow Real). Luminance at the border (and at the surface for the Real condition) was sinusoidally modulated over time (0.5 Hz), with the average luminance always remaining static and equal across the four conditions (Blank condition not shown). The strength of the illusion was more pronounced when modulated in time (unpublished data, a video of these three stimuli can be accessed at http://www.psy.vanderbilt.edu/faculty/roeaw/edgeinduction/CRN.avi).

was directly modulated. In the Cornsweet condition, although there was no actual surface-luminance modulation (both surfaces were equiluminant and static), the modulation of border contrast induced the illusion of surface brightness modulation perceptually equivalent to that of the Real[36] (**Fig. 1c**). Thus, the Cornsweet condition permits the study of edge-induced brightness (due solely to the contrast border) independent of possible confounds from surface luminance contrast or simultaneous contrast. The Narrow Real condition served as a closely matched control for the Cornsweet condition, whereby the border modulation was comparable in magnitude to that of the Cornsweet, but induced a weaker and opposite illusory brightness percept. The Blank baseline condition was an unmodulated homogeneous gray screen[20,37].

Shifts in relative spike timing

We began by asking whether we could observe systematic changes in spike timing between border and surface responses. For each pair of simultaneously recorded spike trains, we generated a cross-correlogram (a histogram of relative timing)[38–43] and quantified the center-of-mass position of the correlogram under each condition (all correlograms were shuffle-corrected for correlated firing that was time-locked to the stimulus; that is, corrected for differences in response latency).

We confirmed that, indeed, visual stimulation can evoke shifts in the relative spike times of border-surface pairs (examples of paired recordings, **Fig. 2**). In comparison with the relative spike timing under Blank conditions (black line), such shifts in peak center-of-mass position were seen under evoked (Real, blue; Cornsweet, red; Narrow Real,

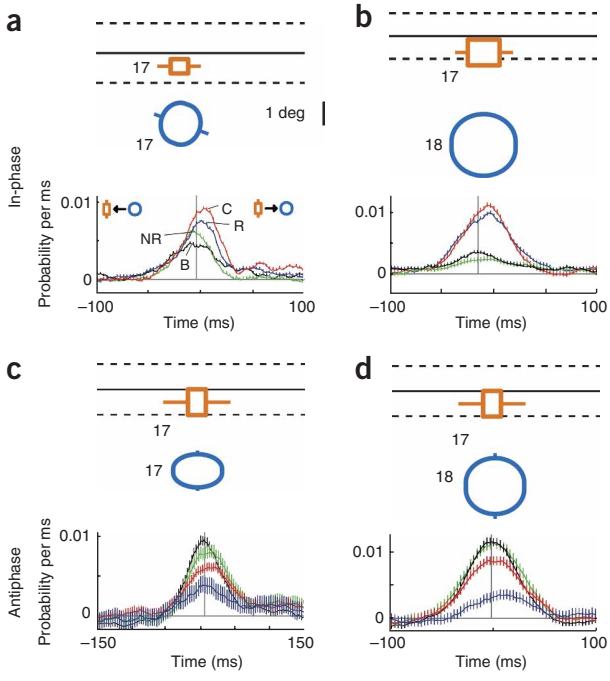

Figure 2 Examples of changes in spike timing interactions for 17–17 and 17-18 cell pairs with in-phase and antiphase relationships. (**a**,**c**) 17–17 pairs. (**b**,**d**) 17–18 pairs. Top, stimuli were positioned such that the border region, consisting of the primary contrast edge (solid line) and extent of Cornsweet (C) and Narrow Real (NR) borders (dashed lines), overlaid the classical receptive field (CRF) of cell 1 (orange) and was away from the CRF of cell 2 (blue). Both CRFs were on the same side of the primary contrast border. Lines on CRFs indicate orientation preference and lengths indicates degree of orientation selectivity (<45° orientation tuning width for border receptive fields). Bottom, cross-correlation histograms showing the frequency of relative spike times under Real (R, blue), Cornsweet (red), Narrow Real (green) and Blank (B, black) conditions. Abscissa indicates spike times of cell 2 (receptive field at surface) following (+) or preceding (–) spike times of cell 1 (receptive field at border). Cross-correlation histograms are corrected for driven rate by normalization and shuffle subtraction. Error bars indicate standard error ($N = 20$) and are asymmetrically distributed. For in-phase pairs ($<\pi/2$ difference in Real response; **a**,**b**), note the inherent surface-to-border directional bias under the Blank condition and positive shifts in peak position and increases in peak height under Real and Cornsweet conditions. Antiphase pairs ($\pi/2$–π difference) (**c**,**d**) showed positive changes in peak position, but decreases in peak height. Peak positions (R, C, NR, B): (**a**) –0.9, 1.7, –5.6, –6.2 ms, (**b**) –8.1, –7.6, –5.7, –12.9 ms, (**c**) 9.0, 13.2*, 13.7*, 6.0 ms, (**d**) 9.0*, 1.8, 0.6, –0.9 ms. Asterisks indicate significant shifts at $P < 0.05$.

green) conditions for '17–17' pairs (**Fig. 2a,c**) and '17–18' pairs (**Fig. 2b,d**). In all four examples, the evoked shifts are in the border-to-surface direction (positive, to the right) relative to the Blank condition. Notably, the evoked peak position could be reversed by swapping the location of the stimulus border over the cell pair (**Fig. 3**), suggesting that the shifts are context-dependent changes in the properties of neurons as they are stimulated by luminance edges and regions of uniform luminance.

Although examples of substantial shifts were found for both border-to-surface (positive) and surface-to-border (negative) directions, shifts were predominantly in the positive direction across the population. Peak positions with Real, Cornsweet and Narrow Real conditions were, on average, positively shifted relative to Blank (**Fig. 4** scatter plots, black dots above the diagonal; solid points are pairs with significant ($P < 0.05$) differences between evoked and baseline conditions, and red error bars indicate the 5–95 percentile bootstrapped distribution for the evoked and baseline conditions). As a population, the shifts were more prominent for 17–18 pairs (**Fig. 4g,i,k**) than they were for 17–17 pairs (**Fig. 4a,c,e**) (for Real, Cornsweet and Narrow Real stimulus conditions: 17–17, $P = 0.6$, 0.071 and 0.14, respectively; 17–18, $P = 6 \times 10^{-7}$, 0.0051 and 0.0004, respectively; paired *t*-test; see **Supplementary Table 1** online for descriptive statistics). The predominance of positive shifts was further supported by binomial comparisons of number of pairs with positive versus negative shifts (**Fig. 4b,d,f,h,j,l**). This was observed, in particular, for 17–18 cell pairs; significant population shifts were observed both for the entire 17–18 sample (Real, $P < 0.0001$; Narrow Real, $P < 0.02$) and for the subpopulation of 17–18 cell pairs with statistically significant peak shifts (**Fig. 4g,i,k**, filled circles; Real, $P < 0.0001$; Narrow Real, $P < 0.001$).

Such shifts were not simply due to differences in response latency, as these effects would have been subtracted out by the shuffle-correction. The shifts are also not simply artifacts of increases in coincident activity driven by common input, as such shifts should be consistently toward zero time difference. Instead, several of the examples (**Fig. 4**) are substantial shifts away from coincident activity (for example, points above diagonal in quadrant 1). These results indicate that, as a population, simple border-contrast stimulus conditions can induce a shift of relative border/surface activation.

Relative spike timing: phase, stimulus and areal specificity

To determine whether this shift in spike timing was indeed related to border contrast and not simply the result of nonspecific spreading of border-evoked activity[17,19,31], we examined changes in correlogram peak position and peak height. Peak height quantifies the frequency of spike co-occurrence and, as such, reflects the strength of interaction between neurons. We predicted that correlogram peak height should be

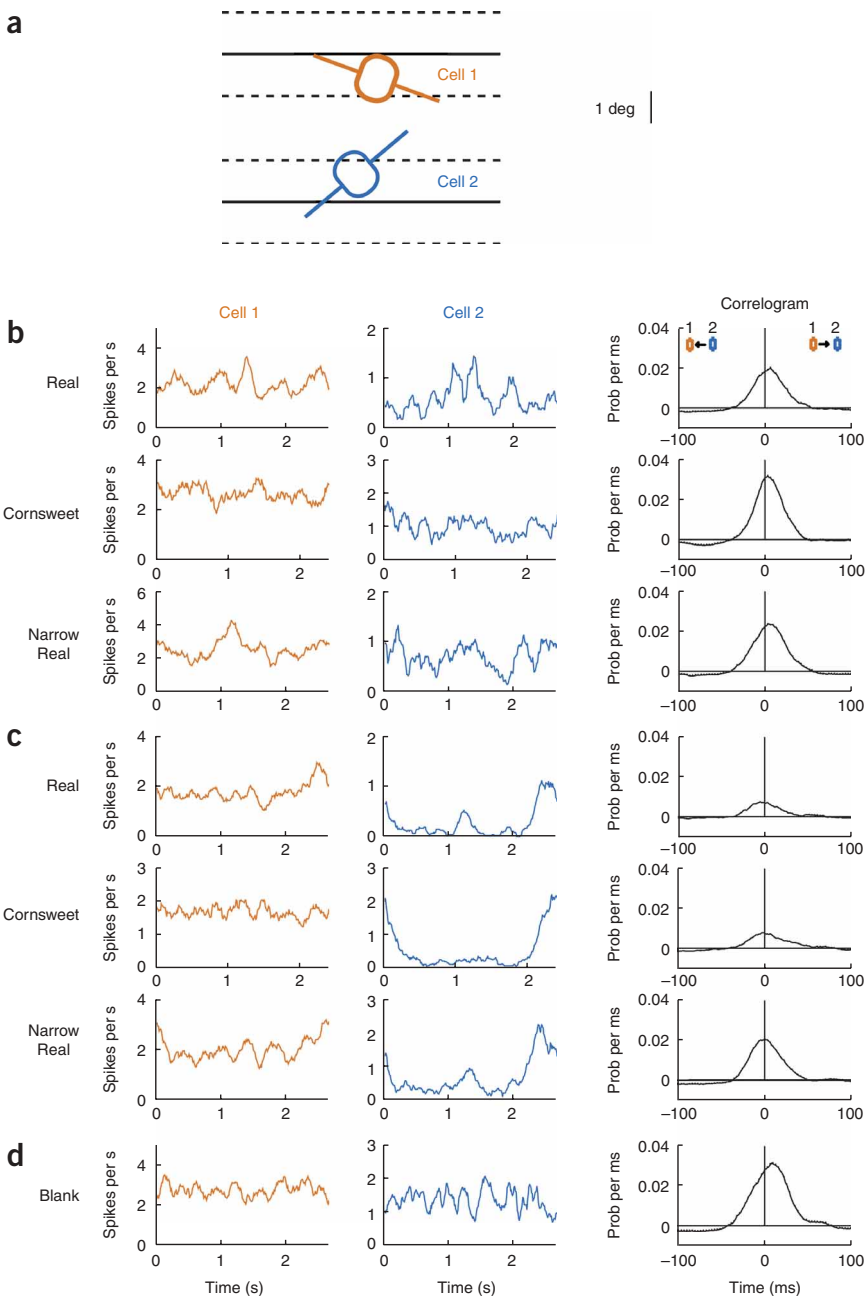

Figure 3 Example of reversal of peak position with border swap. (**a**) Receptive fields of area 17 cells 1 (orange) and 2 (blue) with respect to Real border (horizontal black line) and extent of Cornsweet and Narrow Real borders (dashed lines). (**b**) Peristimulus time histograms (PSTH) and correlogram responses to stimulation with border at cell 1 only. Ordinate in correlograms is in units of probability per ms. Peak positions for R, C and NR are 2.96, 3.91 and 7.83 ms, respectively. Mean, 4.9 ms. (**c**) PSTH and correlogram responses to stimulation with border at cell 2 only. Peak positions for R, C and NR are –2.75, –2.2 and –1.74 ms, respectively. Mean, –2.2 ms. Border position significantly affects peak position (two-tailed paired *t*-test, $t_2 = 4.303$, $P = 0.028$). (**d**) Blank condition. Correlogram shows an inherent 12.3 ms cell 1–to–cell 2 bias in spike times.

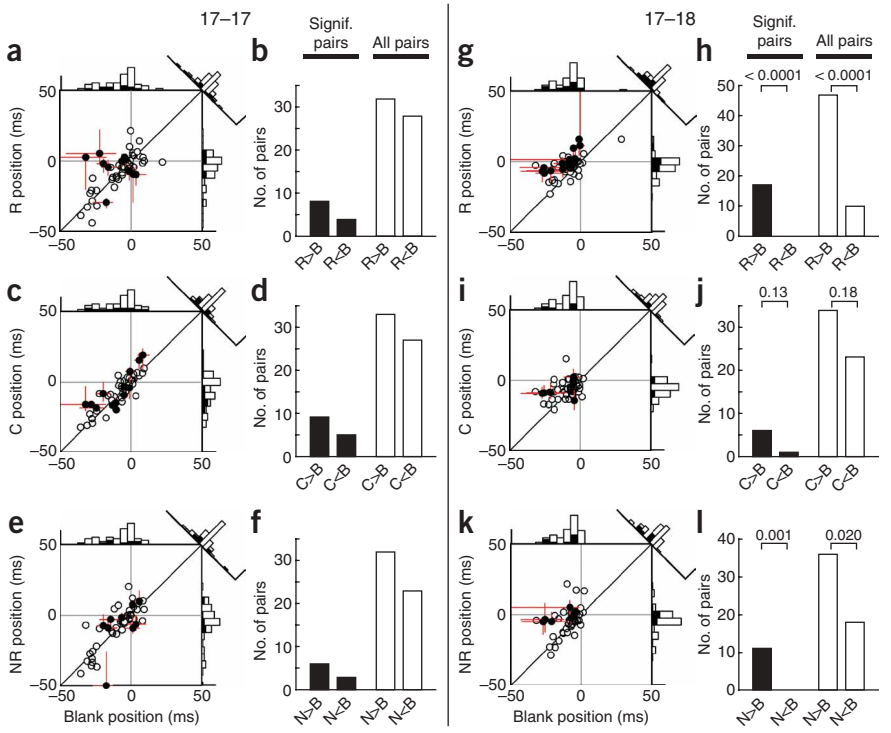

Figure 4 Peak center-of-mass positions are shifted in the border-to-surface direction. (**a**–**l**) Measurements of peak center-of-mass position are shown for the population of 17–17 (**a**–**f**) and 17–18 (**g**–**l**) pairs. Scatter plots compare center-of-mass positions in evoked conditions (R, C, NR) against baseline (Blank). Deviations from the diagonal indicate changes in relative spike timing between conditions. Pairs with significant ($P < 0.05$) differences between evoked and baseline conditions are indicated by filled circles and 5–95% error bars (red lines), as determined by bootstrap analyses computed from random cycles. For clarity, plots are clipped at ± 50 ms. Above and to the right of each scatter plot are histograms of the timing relationships for baseline and evoked conditions (5-ms bins, significant shifts with $P < 0.05$ are indicated by solid bars, lengths of lines at ± 50 ms correspond to 10 pairs). Note that baseline interactions were strongly biased in the surface-to-border direction (negative positions). Total number of pairs does not coincide across the three conditions, as not all pairs showed peaks with significant height under all conditions. Bar plots indicate number of pairs with positive border-to-surface (for example, R > B) and negative surface-to-border (for example, R < B) shifts in peak position, relative to baseline. Dark bars indicate pairs with significant shifts $P < 0.05$. Numbers above bars indicate significance of difference in number of pairs with positive versus negative shifts (two-tailed binomial test; significance values based on paired *t*-test are given in main text). Significant shifts in the border-to-surface direction (R > B, C > B, *N* > B) were more evident for 17–18 pairs.

greater for border and surface pairs that prefer the same sign of surface brightness contrast across the stimulus border (that is, a cell at the border preferring dark on the left and light on the right should interact with dark-preferring cells to its left and light-preferring cells to its right, but not vice versa). We therefore split the population into two groups, consisting of 'in-phase' and 'antiphase' pairs, depending on whether the cells' Real responses were in-phase ($< \pi/2$ difference) or out of phase ($[\pi/2] - \pi$ difference) (see Methods). Specifically, we expected that although both in-phase and antiphase pairs may show border-to-surface shifts in relative timing (as a result of the nonspecific spreading of excitability or activity), border-surface interactions should be stronger for in-phase pairs than for antiphase pairs.

In addition to phase-pairing, we also tested whether the interaction strength might depend on the visual stimulus. If the interaction strength is related to edge induction, peak height should be similar under the Real and Cornsweet conditions for in-phase pairs. Under the Narrow Real condition, although the primary border contrast was identical in sign and similar in magnitude to the Real and Cornsweet, the perceived surface brightness contrast was reversed and weaker. This difference in surface brightness percept led us to hypothesize that the interaction strength might be weaker (and peak height smaller) under the Narrow Real condition compared with the Real and Cornsweet conditions.

Examples of changes in interaction strength for in-phase versus antiphase pairs can be seen in **Figure 2**. Although all four examples showed border-to-surface shifts under Real and Cornsweet conditions, such shifts coincided with opposite changes in peak height for in-phase versus antiphase pairs. In-phase pairs (**Fig. 2a**,**b**) showed increases in peak height (red and blue peaks are higher than black baseline peaks), indicating increases in the likelihood of coincident activity under Real and Cornsweet conditions relative to the Blank baseline condition. Antiphase pairs (**Fig. 2c**,**d**) showed decreases in peak height (red and blue peaks are smaller than black peaks), indicating decreases in the likelihood of coincident activity under the same conditions. Furthermore, the changes in peak height were weakest under the Narrow Real condition (green lines), consistent with the weaker Narrow Real brightness illusion. Thus, visual stimulation of in-phase cell pairs resulted in an increased prevalence of border-to-surface interactions, whereas antiphase cell pairs showed relatively decreased border-to-surface interactions.

These patterns are reflected in the population (as shown in **Fig. 4**) and are supported by a generalized linear model (**Supplementary Tables 2–5** online). We expected that interactions would be weakest under the Narrow Real condition. This was indeed the case for 17–18 border-to-surface interactions, regardless of whether the measure was change in peak height or change in coincidence (**Supplementary Table 3**, columns A–D, bottom rows). In the Narrow Real condition, average change in peak height was 112% above that in the Blank condition (compare with Cornsweet condition, 151% above; Real condition, 200% above; **Fig. 5** and **Supplementary Table 3**, column B, balanced design; that is, the same cell pairs, with significant ($P < 0.05$) peak height under all four conditions). These changes for in-phase pairs were significant ($P < 0.0012$, degrees of freedom = 19) compared with antiphase pairs, which were on average unchanged or reduced (Real condition, mean of –22.8% and median of –26.5%) below baseline. Changes in peak height were much weaker and were nonsignificant for 17–17 interactions (**Supplementary Table 3**, top rows). The results were similar when measured in terms of the number of pairs showing increases versus decreases in peak height (data not shown). Overall, these border-to-surface shifts in interactions and increases in the strength of such interactions for in-phase pairs suggest a specific functional circuitry between border and surface responses that may underlie edge induction.

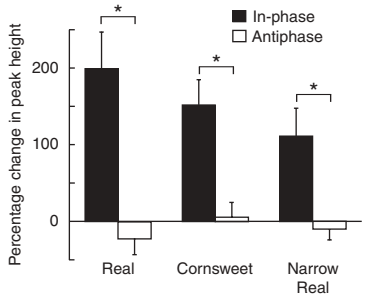

Figure 5 Interactions are strengthened for 17–18 in-phase pairs. Bars show mean ± s.e.m. percent change in peak height for 17–18 in-phase (black, $n = 12$) and antiphase (white, $n = 9$) pairs showing border-to-surface interactions. Peak heights were significantly increased ($P < 0.002$) for in-phase versus antiphase pairs under all conditions.

These findings are bolstered by the fact that the increases in 17–18 in-phase interactions were strongest under the Real and Cornsweet conditions and weakest under the Narrow Real condition, as predicted by the match/mismatch between border and surface brightness contrast in these stimuli.

These shifts are not simply due to uncorrected artifacts of the driven activity. All of our correlograms were normalized for spike count (divided by the lengths of both spike trains) and corrected for stimulus-evoked changes in driven rate by shuffle subtraction. Our findings are thus not simply the result of overall or stimulus-associated differences in latency or responsivity. Correction for slow trial-by-trial covariations in excitability and latency[44] did not substantially affect the results (**Supplementary Tables 4** and **5**). Finally, we considered that feedback from higher areas may explain our findings. As the largest average peak shift for 17–18 pairs was 6.5 ms (**Supplementary Table 1**, in-phase Real versus Blank; corrections apply over the entire time frame of the response at 0.1 ms resolution), if feedback has a role, it would have to operate on a faster timescale.

DISCUSSION

We report here four main results. First, we found context-dependent shifts in the relative timing of visual cortical neurons in the border-to-surface direction under conditions of edge induction. Second, such border-to-surface interactions were strengthened in pairs with matching contrast preferences (in-phase pairs; that is, pairs that would be expected to underlie edge induction). Third, such changes in the relative spike timing were strongest under the Real and Cornsweet conditions and were weakest under the Narrow Real condition, which is consistent with differences in their strength of edge induction. Finally, these effects were stronger in the 17–18 than in the 17–17 interactions. The fact that the 17–18 interactions were significantly phase specific and stimulus-condition specific, but that 17–17 interactions were not, suggests a mechanism for edge induction that is not simply due to the general latency difference between 17–18 and 17–17 interactions. These results are the first evidence that similar circuitry, and in particular 17–18 circuitry, may underlie edge induction in both the Cornsweet brightness illusion and the Real brightness contrast percepts.

Our results suggest a functional linkage (one which we hypothesize to be via horizontal or interareal projections) between border and surface responses in visual cortex underlying the phenomenon of edge induction. In comparison with the baseline condition when the border is not present, a border-to-surface shift in the balance of spike timing emerges under evoked conditions. Thus, the temporal patterns of spike firing between border and surface responses depend on the presence or absence of the contrast border. In effect, it suggests that when we look around the visual world our perception of border-defined objects may be mediated by changes in the relative temporal activation, and not merely the firing rate, of cortical neuronal populations.

Our results provide important quantitative constraints for both the filling-in model (also known as the isomorphic model, where the representation of brightness is propagated across the cortical surface)[5–7] and for models using banks of spatial frequency filters[8–13]. In the filling-in model, one would expect to observe a delayed increase in activity encoding the center of a surface. There is some evidence of such contextual processing of brightness in macaque V1 (refs. 17,19,45,46), although such cases have been limited to observations of single cells and not to how cells interact in concert in a functional circuit. Previous data also have not demonstrated the same degree of stimulus- and cell-specificity of contextual interactions. In our data, 17–17 interactions clearly showed a border-to-surface delay at longer distances; however, changes in the interaction strength with phase were nonsignificant, suggesting a lack of correlation with perception. Furthermore, we have previously reported that area 18 surface responses matched the sign of the perceived edge-induced brightness, consistent with the brightness percepts obtained with both the Real and Cornsweet conditions[20]. In sum, our observations favor a feedforward-dominated 17–18 model of edge-to-surface propagation and emphasize the importance of interareal interactions in the integration of border and surface information. We believe that this finding is biologically important, as it pinpoints a location (the first stages of visual cortex) and a specific putative circuitry (17–18) underlying the psychophysical phenomenon of edge induction.

METHODS

Responses of well-isolated single units were recorded from eight cats according to a protocol approved by the Yale University Institutional Animal Care and Use Committee. Animals were anesthetized with sodium pentothal and eyes immobilized with vecuronium bromide, converged and focused on a CRT monitor (60 Hz, 28–145-cm distance)[20]. The boundary between areas 17 and 18 was mapped by optical imaging and electrophysiology. Cell pairs were selected and characterized on the basis of audible response to a uniform luminance region ($5^\circ \times 5^\circ$) and oriented ($2^\circ \times 0.3^\circ$) stimuli controlled from a handheld light gun. The first cell in each pair was selected for substantial firing-rate modulation by the uniform luminance region (surface) of the Real stimulus positioned over its receptive field (15% peak-peak contrast, 0.5-Hz sinusoidal modulation contrast-reversing across a stationary border; see ref. 20). Peak-peak contrast for Cornsweet and Narrow Real stimuli were 30% and 15%, respectively. In humans, these levels yield comparable strengths of brightness percept for Real and Cornsweet stimuli and a weaker percept for the Narrow Real stimulus[36] (unpublished data, http://www.psy.vanderbilt.edu/faculty/roeaw/edgeinduction). The second cell in each pair was isolated on the basis of response to an oriented bar orthogonal to the location of the receptive field of the first cell (see **Supplementary Figs. 1–4** online). Although cats possess comparable retinogeniculocortical organization and have been shown to perceive subjective contours[47,48], it is possible that cats do not perceive edge-induced brightness the way humans do. Stimuli were positioned such that both receptive fields lay on the same side of the primary contrast border (that is, same surface; as shown in **Fig. 2**). Cornsweet and Narrow Real border regions extended 1° from the primary contrast edge, and the nearest edge of the distant receptive field (at the stimulus surface) was $2–5^\circ$ from the primary contrast edge. Although the border was far from the distant receptive field, it was nonetheless able to modulate the cell's firing rate via the extraclassical receptive field as we previously reported[20]. Each stimulus was presented continuously for approximately 10 min, or until >3,000 spikes were collected. Such long presentations were necessary to reliably compute cell-pair interactions under these conditions and did not noticeably affect the strength of the percept, although the strength of the percept could be modulated by attention to or away

from the surfaces. Response phase was measured by fitting a sinusoid, matching the temporal frequency of the stimulus, to the peristimulus time histogram. All test statistics were two-tailed, using a significance level of 0.05, and were corrected for multiple comparisons where applicable. Additional information can be found in the **Supplementary Methods** online.

Note: Supplementary information is available on the Nature Neuroscience website.

ACKNOWLEDGMENTS

We wish to thank F.L. Healy for technical assistance, Y.-T. Wu for statistical support and S.-S. Huang for helpful discussions. We also thank E.H. Adelson, G. Kreiman and H. Op de Beeck for helpful comments on an earlier version of the manuscript. The project was supported by US National Institutes of Health grants EY-11744, NEI 5T32 EY-07115, 5T32 DA-07290 and RR-15574, the Whitehall Foundation, Packard Foundation, Yale Brown-Coxe Postdoctoral Fellowship, Taiwan Ministry of Education Five Year Aim for the Top University Plan, and the Taiwan National Science Council and Ministry of Education Outstanding Scholar Fellowship 95-2819-B-010-001.

AUTHOR CONTRIBUTIONS

C.P.H. and A.W.R. designed the experiments. C.P.H., B.M.R. and A.W.R. carried out the experiments and wrote the paper. C.P.H. analyzed the results.

COMPETING INTERESTS STATEMENT

The authors declare no competing financial interests.

Published online at http://www.nature.com/natureneuroscience
Reprints and permissions information is available online at http://npg.nature.com/reprintsandpermissions

1. Cornsweet, T.N. *Visual Perception* (Academic, New York, 1970).
2. Mumford, D., Kosslyn, S.M., Hillger, L.A. & Herrnstein, R.J. Discriminating figure from ground: the role of edge detection and region growing. *Proc. Natl. Acad. Sci. USA* **84**, 7354–7358 (1987).
3. Adelson, E.H. Perceptual organization and the judgment of brightness. *Science* **262**, 2042–2044 (1993).
4. Anderson, B.L. & Winawer, J. Image segmentation and lightness perception. *Nature* **434**, 79–83 (2005).
5. Zucker, S.W. in *The Encyclopedia of Artificial Intelligence* (ed. Shapiro, S.) (John Wiley, New York, 1986).
6. Elder, J.H. & Zucker, S.W. Evidence for boundary-specific grouping. *Vision Res.* **38**, 143–152 (1998).
7. Grossberg, S. & Hong, S. A neural model of surface perception: lightness, anchoring, and filling-in. *Spat Vis.* **19**, 263–321 (2006).
8. Blakeslee, B., Pasieka, W. & McCourt, M.E. Oriented multiscale spatial filtering and contrast normalization: a parsimonious model of brightness induction in a continuum of stimuli including White, Howe and simultaneous brightness contrast. *Vision Res.* **45**, 607–615 (2005).
9. Dakin, S.C. & Bex, P.J. Natural image statistics mediate brightness 'filling in'. *Proc. Biol. Sci.* **270**, 2341–2348 (2003).
10. Purves, D., Shimpi, A. & Lotto, R.B. An empirical explanation of the Cornsweet effect. *J. Neurosci.* **19**, 8542–8551 (1999).
11. Komatsu, H., Kinoshita, M. & Murakami, I. Responses in the retinotopic representation of the blind spot in the macaque V1 to stimuli for perceptual filling-in. *J. Neurosci.* **20**, 9310–9319 (2000).
12. Pessoa, L., Thompson, E. & Noë, A. Finding out about filling-in: a guide to perceptual completion for visual science and the philosophy of perception. *Behav. Brain Sci.* **21**, 723–748 discussion 748–802 (1998).
13. Komatsu, H. Surface representation by population coding. *Behav. Brain Sci.* **21**, 761–762 (1998).
14. Davey, M.P., Maddess, T. & Srinivasan, M.V. The spatiotemporal properties of the Craik-O'Brien-Cornsweet effect are consistent with 'filling-in'. *Vision Res.* **38**, 2037–2046 (1998).
15. Paradiso, M.A. & Hahn, S. Filling-in percepts produced by luminance modulation. *Vision Res.* **36**, 2657–2663 (1996).
16. Paradiso, M.A. Visual neuroscience: illuminating the dark corners. *Curr. Biol.* **10**, R15–R18 (2000).
17. De Weerd, P., Gattass, R., Desimone, R. & Ungerleider, L.G. Responses of cells in monkey visual cortex during perceptual filling-in of an artificial scotoma. *Nature* **377**, 731–734 (1995).
18. Rossi, A.F., Rittenhouse, C.D. & Paradiso, M.A. The representation of brightness in primary visual cortex. *Science* **273**, 1104–1107 (1996).
19. Lamme, V.A.F., Rodriguez-Rodriguez, V. & Spekreijse, H. Separate processing dynamics for texture elements, boundaries and surfaces in primary visual cortex of the macaque monkey. *Cereb. Cortex.* **9**, 406–413 (1999).
20. Hung, C.P., Ramsden, B.M., Chen, L.M. & Roe, A.W. Building surfaces from borders in areas 17 and 18 of the cat. *Vision Res.* **41**, 1389–1407 (2001).
21. Roe, A.W., Lu, H.D. & Hung, C.P. Cortical processing of a brightness illusion. *Proc. Natl. Acad. Sci. USA* **102**, 3869–3874 (2005).
22. Bonhoeffer, T., Kim, D-S., Malonek, D., Shoham, D. & Grinvald, A. Optical imaging of the layout of functional domains in area 17 and across the area 17/18 border in cat visual cortex. *Eur. J. Neurosci.* **7**, 1973–1988 (1995).
23. Bredfeldt, C.E. & Ringach, D.L. Dynamics of spatial frequency tuning in macaque V1. *J. Neurosci.* **22**, 1976–1984 (2002).
24. Cavanaugh, J.R., Bair, W. & Movshon, J.A. Nature and interaction of signals from the receptive field center and surround in macaque v1 neurons. *J. Neurophysiol.* **88**, 2530–2546 (2002).
25. DeAngelis, G.C., Freeman, R.D. & Ohzawa, I. Length and width tuning of neurons in the cat's primary visual cortex. *J. Neurophysiol.* **71**, 347–374 (1994).
26. Ferster, D. & Jagadeesh, B. Nonlinearity of spatial summation in simple cells of areas 17 and 18 of cat visual cortex. *J. Neurophysiol.* **66**, 1667–1679 (1991).
27. Issa, N.P., Trepel, C. & Stryker, M.P. Spatial frequency maps in cat visual cortex. *J. Neurosci.* **20**, 8504–8514 (2000).
28. Shoham, D., Hubener, M., Schulze, S., Grinvald, A. & Bonhoeffer, T. Spatio-temporal frequency domains and their relation to cytochrome oxidase staining in cat visual cortex. *Nature* **385**, 529–533 (1997).
29. Zhou, H., Friedman, H.S. & von der Heydt, R. Coding of border ownership in monkey visual cortex. *J. Neurosci.* **20**, 6594–6611 (2000).
30. Sceniak, M.P., Ringach, D.L., Hawken, M.J. & Shapley, R. Contrast's effect on spatial summation by macaque V1 neurons. *Nat. Neurosci.* **2**, 733–739 (1999).
31. Rossi, A.F., Desimone, R. & Ungerleider, L.G. Contextual modulation in primary visual cortex of macaques. *J. Neurosci.* **21**, 1698–1709 (2001).
32. Reid, R.C. & Alonso, J.M. Specificity of monosynaptic connections from thalamus to visual cortex. *Nature* **378**, 281–284 (1995).
33. Bullier, J. & Henry, G.H. Neural path taken by afferent streams in striate cortex of the cat. *J. Neurophysiol.* **42**, 1264–1270 (1979).
34. Givre, S.J., Schroeder, C.E. & Arezzo, J.C. Contribution of extrastriate area V4 to the surface-recorded flash VEP in the awake macaque. *Vision Res.* **34**, 415–428 (1994).
35. Schyns, P.G. & Oliva, A. From blobs to boundary edges: evidence for time- and spatial-scale–dependent scene recognition. *Psychol. Sci.* **5**, 195–200 (1994).
36. Burr, D.C. Implications of the Craik-O'Brien illusion for brightness perception. *Vision Res.* **27**, 1903–1913 (1987).
37. Hung, C.P., Ramsden, B.M. & Roe, A.W. Weakly modulated spike trains: significance, precision and correction for sample size. *J. Neurophysiol.* **87**, 2542–2554 (2002).
38. Nowak, L.G., Munk, M.H.J., Nelson, J.I., James, A.C. & Bullier, J. Structural basis of cortical synchronization. I. Three types of interhemispheric coupling. *J. Neurophysiol.* **74**, 2379–2400 (1995).
39. Alonso, J.-M. & Martinez, L.M. Functional connectivity between simple cells and complex cells in cat striate cortex. *Nat. Neurosci.* **1**, 395–403 (1998).
40. Das, A. & Gilbert, C.D. Topography of contextual modulations mediated by short-range interactions in primary visual cortex. *Nature* **399**, 655–661 (1999).
41. Siegel, M. & Konig, P. A functional gamma-band defined by stimulus-dependent synchronization in area 18 of awake behaving cats. *J. Neurosci.* **23**, 4251–4260 (2003).
42. Singer, W. Neuronal synchrony: a versatile code for the definition of relations? *Neuron* **24**, 49–65 111–25 (1999).
43. Ts'o, D.Y., Gilbert, C.D. & Wiesel, T.N. Relationships between horizontal interactions and functional architecture in cat striate cortex as revealed by cross-correlation analysis. *J. Neurosci.* **6**, 1160–1170 (1986).
44. Brody, C.D. Correlations without synchrony. *Neural Comput.* **11**, 1537–1551 (1999).
45. Kinoshita, M. & Komatsu, H. Neural representation of the luminance and brightness of a uniform surface in the macaque primary visual cortex. *J. Neurophysiol.* **86**, 2559–2570 (2001).
46. MacEvoy, S.P., Kim, W. & Paradiso, M.A. Integration of surface information in primary visual cortex. *Nat. Neurosci.* **1**, 616–620 (1998).
47. Bravo, M., Blake, R. & Morrison, S. Cats see subjective contours. *Vision Res.* **28**, 861–865 (1988).
48. De Weerd, P., Sprague, J.M., Raiguel, S., Vandenbussche, E. & Orban, G.A. Effects of visual cortex lesions on orientation discrimination of illusory contours in the cat. *Eur. J. Neurosci.* **5**, 1695–1710 (1993).